Desalination and Water Treatment
www.deswater.com
doi: 10.5004/dwt.2020.25224

182 (2020) 309–319
April

Electrocatalytic dechlorination of 2,4-dichlorophenoxyacetic acid using a Pd-Co_3O_4/Ni foam electrode: Influencing factors and possible environmental applications

Qiuxiang Liu[a,b], Jinhui Fang[b], Sulin Ni[b], Shasha Tang[b], Zhiqiao He[b,*]

[a]*Collaborative Innovation Center of Yangtze River Delta Region Green Pharmaceuticals, Zhejiang University of Technology, Hangzhou 310032, China, email: 149203760@qq.com (Q. Liu)*
[b]*College of Environment, Zhejiang University of Technology, Hangzhou 310032, China, Tel. 86-571-88320726; Fax: 86-571-88320276; emails: zqhe@zjut.edu.cn (Z. He), jinhuifang1113@163.com (J. Fang), 15988821752@163.com (S. Ni), 614716432@qq.com (S. Tang)*

Received 14 July 2019; Accepted 23 November 2019

ABSTRACT

A hybrid electrode comprised of Pd and Co_3O_4 supported on Ni foam (Pd-Co_3O_4/Ni foam) was applied toward the dechlorination of 2,4-dichlorophenoxyacetic acid (2,4-D). The effects of the reaction condition, such as Co_3O_4 and Pd loading, current density, initial concentration of 2,4-D, temperature and dissolved anions, on the electrochemical dechlorination process were investigated and interpreted based on an indirect reduction mechanism via active atomic H*. The optimal Pd and Co_3O_4 loading were determined to be 0.47 and 0.51 mg/cm^2, respectively. A highest current efficiency of 12.10% was obtained at a current density of 1.50 mA/cm^2, an initial 2,4-D concentration of 50 mg/L and reaction temperature of 298 K, and the apparent activation energy of 2,4-D dechlorination by the Pd-Co_3O_4/Ni foam electrode was calculated to be 42.33 × 10^3 J/mol. In addition, dissolved anions such as S^{2-}, SO_3^{2-} and NO_3^- suppress the catalytic activity, whereas HCO_3^- and Cl^- have a negligible effect on the reaction process. The Pd-Co_3O_4/Ni foam electrode can also be applied to the dechlorination of 2,4-D in natural water bodies as well as other chlorinated organic compounds, such as chlorophenols.

Keywords: Electrocatalytic dechlorination; Pd-Co_3O_4/Ni foam electrode; 2,4-dichlorophenoxyacetic acid; Dissolved anions; Influencing factors

1. Introduction

The ecological risk of potential environmental pollutants has drawn a lot of attention over the last several decades [1–11], and particular attention has been paid to chlorinated organic compounds (COCs). 2,4-Dichlorophenoxyacetic acid (2,4-D) is a typical COC, which is widely used in agriculture and plants and has been detected in water bodies, even at concentrations of several mg/L in large reservoirs [1]. Due to its toxicological effects on living organisms [2], developing efficient methods for the removal of 2,4-D is highly desirable [3,4].

To remove 2,4-D from water, several degradation technologies have been reported, including biological [5,6] and advanced oxidation [8,9] processes. However, these methods usually suffer from several limitations, such as long processing time and secondary pollution. Electrochemical treatment technologies including anodic oxidation [12,13] and cathodic reduction methods [14–16], as a green processing technology, have attracted enormous attention in the field of treating toxic and refractory contaminants in an aqueous solution. The cathodic reduction method has the advantages of rapid reaction rate, low apparatus cost, and mild reaction conditions. When used to treat

* Corresponding author.

halogen-containing pollutants, a cathodic reduction can ensure the selective removal of halogen atoms from COCs without producing toxic by-products or adding any toxic chemicals [17–19].

Pd-, Au- and Ag-modified electrodes have extraordinary electrocatalytic activities for the reduction of COCs [20–22]. Among them, the noble metal catalysts using Pd have been extensively used because the multiple σ-bonding formed between H atoms and the d-orbitals of Pd are beneficial to the generation of active atomic hydrogen (H*) via the dissociation of H_2 inside the Pd lattice [23,24]. However, because Pd is an expensive metal, efforts have been devoted to reducing the amount of Pd by adding other inexpensive conductive materials [18,25]. Our previous studies have confirmed that transition metal oxides such as Co_3O_4 show great potential as co-catalysts to reduce the amount of Pd while maintaining the catalytic activity and enhance the tolerance to catalyst inactivation in the electrochemical dechlorination process [26].

In this work, a Pd and Co_3O_4 hybrid electrode supported on Ni foam (Pd-Co_3O_4/Ni foam) were prepared for the electrochemical reductive dechlorination of 2,4-D. Ni foam was chosen as the electrode substrate due to its advantages of large specific surface area, porous structure and excellent electrical conductivity [27]. The effects of the Co_3O_4 and Pd loading, current density, initial concentration of 2,4-D, temperature and co-existing dissolved anions in natural water were investigated. In addition, the possibility of applying the Pd-Co_3O_4/Ni foam electrode for dechlorinating 2,4-D in natural water bodies and chlorophenols was also studied.

2. Experimental section

2.1. Materials

Ni foam was purchased from Suzhou Jiashide Foam Metal Co. Ltd., China. $PdCl_2$, (59–60% Pd), 2,4-D (≥99%), 2-chlorophenoxyacetic acid (2-CPA, ≥98%), 4-chlorophenoxyacetic acid (4-CPA, ≥98%), phenoxyacetic acid (PA, ≥98%), 2,4-dichlorophenol (2,4-DCP, ≥97%), 2-chlorophenol (2-CP, ≥98%), 4-chlorophenol (4-CP, ≥98%) and phenol (≥97%) were purchased from Aladdin Reagent Inc., China. Nafion-117 membranes were obtained from DuPont de Nemours & Co., USA. Ultrapure water obtained from a Millipore water purification system (Milli-Q) with a specific conductibility of ≥18 mW/cm was used throughout the experiments.

2.2. Electrode preparation and characterization

The Pd-Co_3O_4/Ni foam electrode was prepared as previously described [26,28]. Typically, Ni foam with a fixed size (20 mm × 20 mm × 1.2 mm) was used as the electrode substrate, which was ultrasonically degreased and cleaned for 20 min and immersed in 0.5 mmol/L H_2SO_4 solution for 5 min to remove the surface oxidized layer. Afterward, the Ni foam was washed three times with ultrapure water. The Pd-Co_3O_4/Ni foam electrodes were synthesized via a two-step method of constant potential deposition and calcination. First, the cleaned Ni foam was deposited with Pd and $Co(OH)_2$ at a constant potential of −1.0 V vs. saturated calomel electrode (SCE) for 20 min in 40 mL of an aqueous solution containing 5 mmol/L $Co(NO_3)_2$ and 1 mmol/L $PdCl_2$. Then, the deposited electrode was repeatedly washed with ultrapure water and dried under a flow of N_2. Finally, the material was calcined in a tube furnace at 523 K for 120 min. When studying the optimum loading of Pd and Co_3O_4, the $Co(NO_3)_2$ concentration was varied from 1 to 50 mmol/L, and that of $PdCl_2$ was varied from 0.5 to 2 mmol/L.

The Pd and Co_3O_4 loading on the electrodes was analyzed using inductively coupled plasma-optical emission spectroscopy (ICP-OES; Optima 7000DV, Perkin-Elmer Co. Ltd., USA). The surface morphology of the Pd-Co_3O_4/Ni foam electrode was observed using field emission scanning electron microscopy (FE-SEM; ΣIGMA, Carl Zeiss, Germany). After ultrasonication in ethanol, the detailed morphology and elemental distribution on the surface of the Ni foam electrode were determined using transmission electron microscopy (TEM; Tecnai G2 F30 S-Twin, Philips-FEI Corp., Netherlands) operated at 300 kV.

2.3. Experimental procedure and analysis

A double-chamber glass cell (4 cm × 11 cm) divided by a cationic exchange membrane (Nafion-117) was used for our electrochemical experiments. The cathode compartment contains 30 mL of 2,4-D and a 17 mmol/L Na_2SO_4 solution or other additional anions, which was continuously mixed by a magnetic stirrer during the electrochemical reaction. The anode compartment contains 25 mL of Na_2SO_4. The Pd-Co_3O_4/Ni foam working electrode and SCE reference electrode were placed in the catholyte. A Pt counter electrode (2 cm × 2 cm) was placed in the anolyte. The electrolyte temperature was maintained at a pre-set temperature using a constant temperature water bath (THD-2015, Ningbo Tian Heng Instrument Factory, China). The electrochemical experiments were controlled using an electrochemical workstation (CHI760E, Shanghai Chen Hua Instrument Co., China). 0.4 mL of the sample was withdrawn from the catholyte at pre-set time intervals for further analysis.

The concentrations of 2,4-D, 2-CPA, 4-CPA, PA and phenol were analyzed using high-performance liquid chromatography (HPLC; 1200 series, Agilent Technologies, USA) at 210 nm with an Agilent XDB-C18 column (150 mm × 4.6 mm). The mobile phase consisted of 60:40 methanol-water (0.2% H_3PO_4) at a flow rate of 0.8 mL/min. The injected volume for all samples was 5 μL and the column temperature was 298 K. Calculation of the current efficiency (CE) for 2,4-D dechlorination is described in detail in the literature [15].

3. Results and discussion

3.1. Characterization of the Pd-Co_3O_4/Ni foam electrode

Fig. 1 shows the surface morphology of the Pd-Co_3O_4/Ni foam electrode. The scanning electron microscopy image shows that the as-synthesized electrode possesses a 3D cross-linked structure with hierarchical pore sizes (Fig. 1a) [29]. The hybrid electrode is composed of Co_3O_4 nanosheets and Pd nanoparticles, with Pd uniformly dispersed on the surface of the Co_3O_4 nanosheets. The low-magnification TEM image demonstrates that all of the as-synthesized catalysts are loosely gathered together [30]. The size of the granular Pd is in the range of 20–70 nm with an average size of ~35 nm

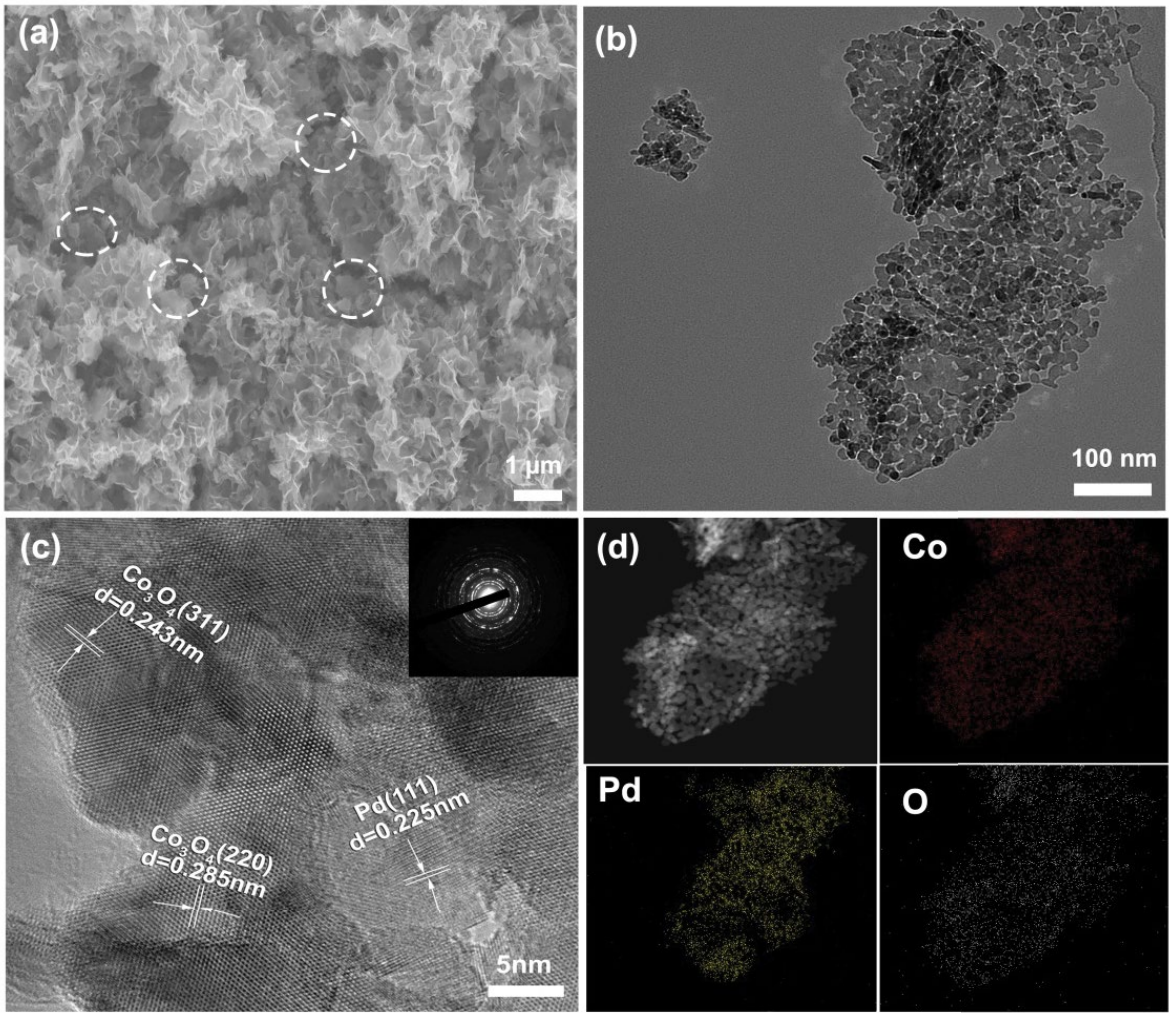

Fig. 1. (a) FE-SEM, (b) TEM, (c) high-resolution TEM (Inset is the selected-area electron diffraction pattern) images, and (d) elemental mapping images of the Pd-Co_3O_4/Ni foam electrode.

(Fig. 1b). The high-resolution TEM image (Fig. 1c) shows a lattice spacing value of 0.225 nm, corresponding to the (111) plane of face-centered cubic Pd [31,32]. Moreover, lattice fringes with a spacing of 0.243 and 0.285 nm corresponding to the (311) and (220) planes of cubic Co_3O_4, respectively, are visible [33,34]. The selected area electron diffraction pattern is shown in the inset of Fig. 1c displays well-defined rings, which further confirm that the sample exhibits a polycrystalline nature. Fig. 1d shows the elemental distribution, in which the Co, O, and Pd signals are overlapped over the entire investigated area, thereby indicating that the Co, O and Pd elements were evenly deposited on the Ni foam. All these results verify that Pd and Co_3O_4 were successfully synthesized on the Ni foam surface.

3.2. Effect of the catalyst composition on the dechlorination of 2,4-D

To determine the role of the Co_3O_4 and Pd loading on the dechlorination of 2,4-D, we used seven types of electrodes for comparison. According to the literature and our previous work [15,18,19], four types of electrodes were prepared at $Co(NO_3)_2$ concentrations of 1, 5, 25 and 50 mmol/L, while keeping the $PdCl_2$ concentration at 1 mmol/L. Three other electrodes were prepared at $PdCl_2$ concentrations of 0.5, 1 and 2 mmol/L while keeping the $Co(NO_3)_2$ concentration at 5 mmol/L. The Pd and Co_3O_4 content in these electrodes are summarized in Table 1.

As shown in Fig. 2a, the removal efficiency toward 2,4-D initially increased and then decreased upon increasing the Co_3O_4 loading. The optimum loading of Co_3O_4 was found to be 0.51 mg/cm^2. This is because the generation and adsorption of atomic H* were accelerated by increasing the Co_3O_4 content. However, excessive Co_3O_4 loading will block the active sites of Pd and suppress the formation of active atomic H*.

Fig. 2b illustrates that at a Pd loading of 0.22, 0.47 and 0.93 mg/cm^2, the removal efficiency toward 2,4-D after 60 min of electrolysis was 59.2%, 94.3%, and 98.8%, respectively. Therefore, an excessive Pd loading on the electrode surface was not crucial for the improvement in the 2,4-D dechlorination efficiency. This because excessive Pd will

Table 1
Pd and Co_3O_4 loading on the electrode analyzed using ICP-OES

Electrode	Total loading on the electrode (mg)		Total loading on the electrode (mg/cm²)	
	Pd	Co_3O_4	Pd	Co_3O_4
1	3.76	0.64	0.47	0.08
2	3.76	4.08	0.47	0.51
3	3.76	22.40	0.47	2.80
4	3.76	31.04	0.47	3.88
5	1.75	4.08	0.22	0.51
6	7.45	4.08	0.93	0.51

cause a reduction in the number of available sites as a result of agglomeration. This result was consistent with the findings of our previous research [25].

3.3. Effect of the reaction parameters on the dechlorination of 2,4-D

3.3.1. Current density and pH

The applied current density has been proved to be a crucial parameter in controlling electron transfer and active atomic H* production via water electrolysis during electrochemical dechlorination [19,35], thereby directly influencing the removal efficiency toward 2,4-D. As shown in Fig. 3a, the removal efficiency toward 2,4-D increased as the applied current density increased from 0.50 to 1.50 mA/cm². Further increasing the current density resulted in a slight decrease in dechlorination efficiency. As shown in Fig. 3b, the dechlorination of 2,4-D followed a pseudo-first-order kinetic model, which can be expressed as follows:

$$-\ln\left(\frac{C_t}{C_0}\right) = k_{obs}t + b \quad (1)$$

where t is the reaction time (min), k_{obs} is the observed rate constant (min^{-1}), b is a constant, and C_t and C_0 are the concentration of 2,4-D (mmol/L) at time = t and 0, respectively.

The k_{obs} value increased from 0.004 to 0.062 min^{-1}, and then slightly decreased to 0.041 min^{-1} upon increasing the applied current in the range studied. This result may be attributed to the fact that the hydrogen evolution reaction (HER) can be accelerated at high current density. Correspondingly, the generation of active atomic H* on the surface of the electrode was enhanced, which in turn boosts the electrochemical reduction of 2,4-D. However, in the case when the current density was increased to 2.50 mA/cm², a large amount of H_2 gas was generated on the cathode surface, which impedes the removal of 2,4-D. Thus, a current density of 1.50 mA/cm² was selected as the optimum current density to ensure an improved dechlorination efficiency.

CE is an important factor for determining the number of electrons exhausted during the removal of 2,4-D. Fig. 3c shows the CE gradually increases to 5.50% with no peak value at a current density of 0.50 mA/cm² during the reaction. In contrast, in the current density range of 0.75–2.50 mA/cm², the CE for dechlorination first increases and then decreases, and the maximum CE value was obtained at 30 min. This may be because active atomic H* is mainly consumed to reach an equilibrium between hydrogen in the solid solution phase (PdHx) and hydrogen in the metal hydride phase (PdHy) during the first 30 min. Consequently, HER was accelerated due to the low consumption of active atomic H* by the residual 2,4-D [25,36]. This can also be used to explain the result that a slightly decreased CE of dechlorination was achieved when the current density was increased to 2.50 mA/cm². In this work, the highest CE of 12.10% was got at a current density of 1.50 mA/cm².

The pH is an important factor affecting electrochemical dechlorination [37]. Consequently, the pH changes in the catholyte were monitored, as shown in Fig. 3d. The initial pH of the catholyte was 3.80, which was ascribed to the carboxyl group in the 2,4-D structure. Since the anodic and cathodic compartments are separated by a cation-exchange membrane. The catholyte rapidly becomes basic after

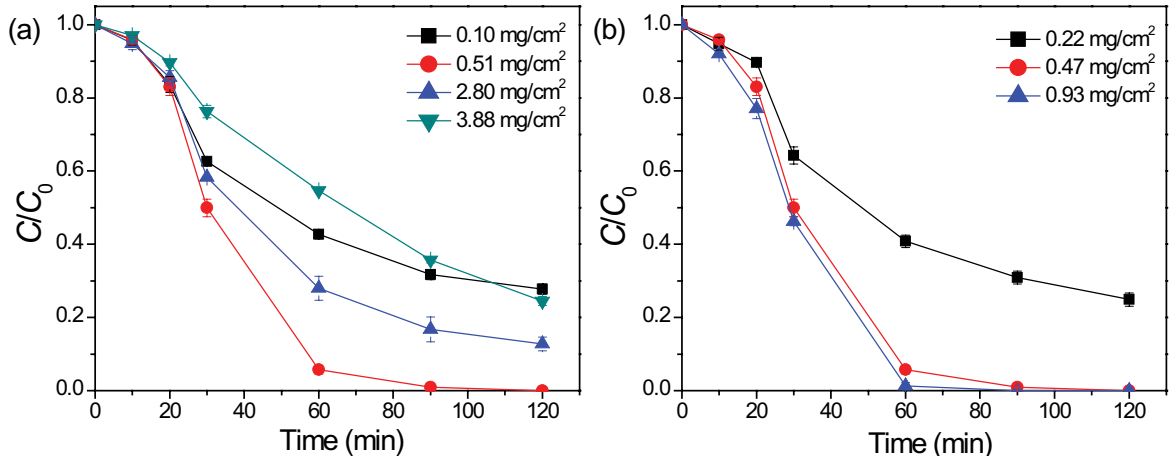

Fig. 2. Effect of the (a) Co_3O_4 and (b) Pd loading in the Pd-Co_3O_4/Ni foam electrode on the dechlorination efficiency toward 2,4-D. Experimental conditions: fixed Pd loading = 0.47 mg/cm², fixed in (a) Co_3O_4 loading = 0.51 mg/cm² in (b), initial 2,4-D concentration = 50 mg/L, applied current density = 1.50 mA/cm², Na_2SO_4 = 17 mmol/L, and reaction temperature = 298 K.

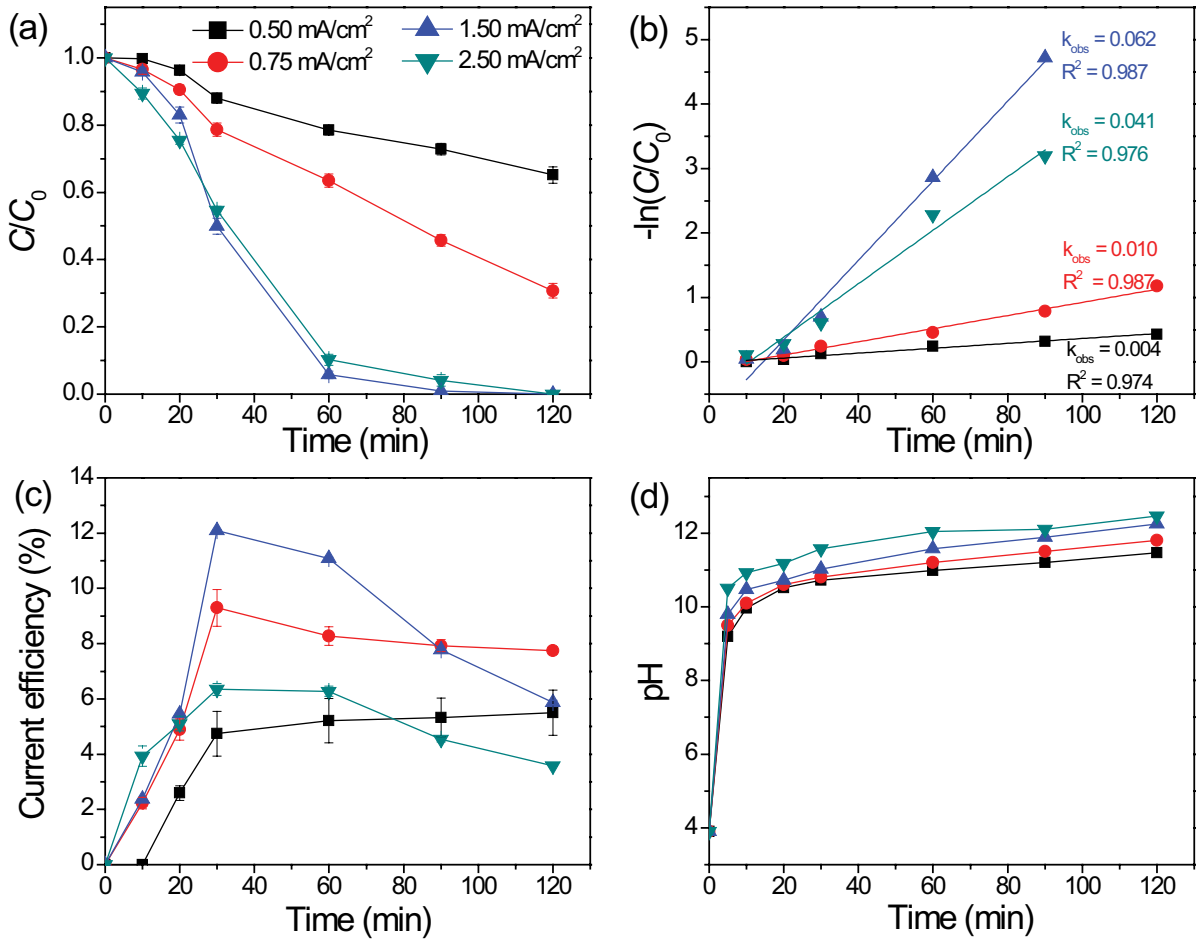

Fig. 3. (a) Effect of the current density on the dechlorination of 2,4-D. (b) Pseudo-first-order fitting of the 2,4-D dechlorination process. (c) Current efficiency and (d) pH changes observed using the Pd-Co_3O_4/Ni foam electrode. Experimental conditions: Pd loading = 0.47 mg/cm^2, Co_3O_4 loading = 0.51 mg/cm^2, initial 2,4-D concentration = 50 mg/L, Na_2SO_4 = 17 mmol/L, and reaction temperature = 298 K.

10 min of electrolysis because of the accumulation of OH^- in the cathode compartment. Afterward, the pH value slowly increases. The final values were 11.47, 11.80, 12.25, and 12.47 at current densities of 0.50, 0.75, 1.50, and 2.50 mA/cm^2 over 120 min of reaction, respectively. In general, a relatively low pH value favors the electrochemical hydrodechlorination process, according to the Nernst equation [25]. In this study, the poor catalytic activity of the Pd-Co_3O_4/Ni foam electrode observed during the beginning of the reaction was attributed to the establishment of a hydrogen adsorption equilibrium in the Pd lattice between PdHx and PdHy.

3.3.2. Initial 2,4-D concentration

To evaluate the effect of the 2,4-D concentration on the dechlorination process, we performed the electrochemical dechlorination experiment using different initial concentrations of 2,4-D (25, 50, 75, and 100 mg/L). Fig. 4a presents the typical carbon balance of 2,4-D dechlorination at an initial concentration of 100 mg/L. 2,4-D was observed to be almost completely transformed into the final product PA. The partially dechlorinated intermediate product 2-CPA was transiently formed at low concentrations before being completely dechlorinated and almost no 4-CPA was detected throughout the electrolysis. The total carbon mass, which represents the evaluation of the total molar amounts of 2,4-D, 2-CPA, 4-CPA, and PA, remained stable during the entire dechlorination process. We can, therefore, conclude that the adsorption of the reactants and products on the electrode surface was negligible.

As shown in Fig. 4b, the 2,4-D concentration decreases significantly upon prolonging the reaction time. More than 96.5% of 2,4-D was removed within 120 min. When the initial concentration was increased from 25 to 100 mg/L, the removal efficiency of 2,4-D was slightly reduced from 100% to 96.5%, and the 2,4-D dechlorination reaction followed a pseudo-first-order kinetic model (Eq. (1)). The k_{obs} value for 2,4-D by the Pd-Co_3O_4/Ni foam electrode decreased from 0.068 to 0.030 min^{-1} when the initial concentration increased from 25 to 100 mg/L. However, the amount of 2,4-D removed increased upon increasing the initial 2,4-D concentration (Fig. 4d). This is because more 2,4-D can be transferred onto the electrode surface for dechlorination at a relatively higher initial concentration [38].

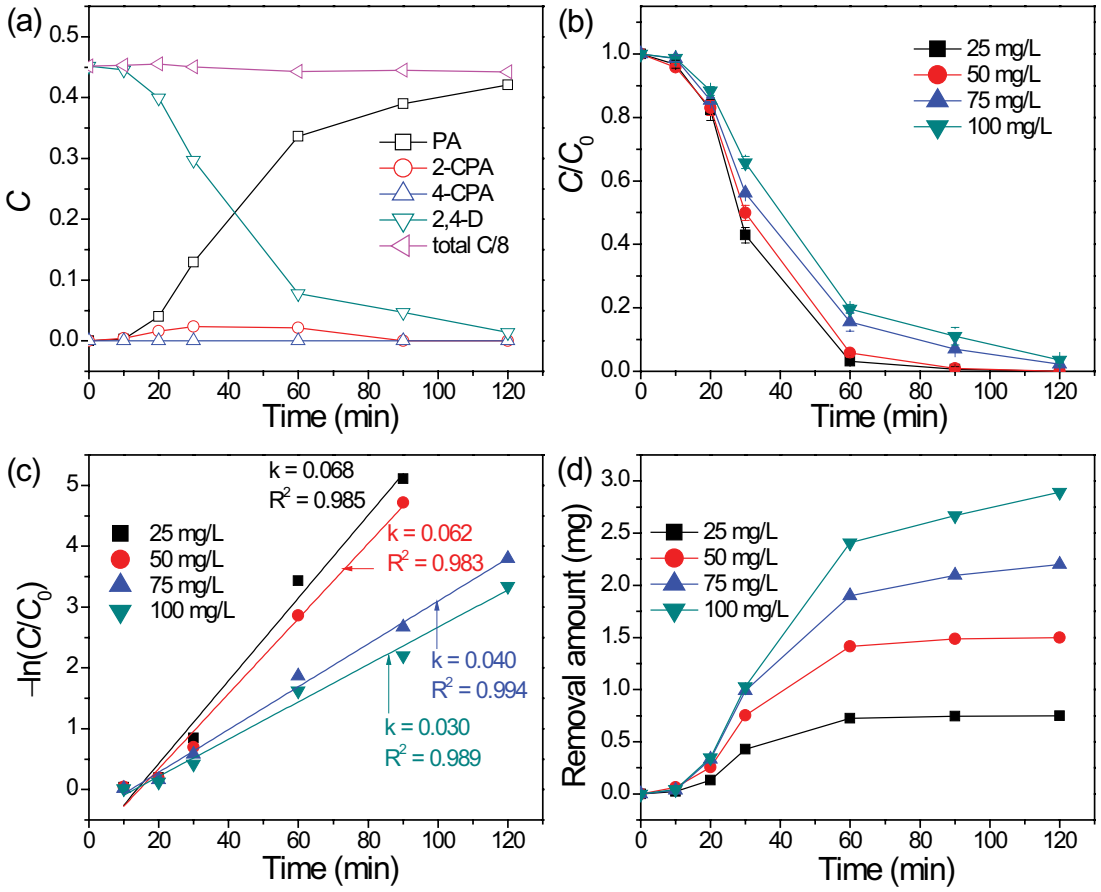

Fig. 4. (a) Time dependence of 2,4-D, intermediate, final product and total carbon concentration at an initial 2,4-D concentration of 100 mg/L. (b) Effect of the initial concentration on the dechlorination of 2,4-D. (c) Pseudo-first-order fitting and (d) removal of 2,4-D using the Pd-Co_3O_4/Ni foam electrode. Experimental conditions: Pd loading = 0.47 mg/cm^2, Co_3O_4 loading = 0.51 mg/cm^2, Na_2SO_4 = 17 mmol/L, applied current density = 1.50 mA/cm^2, and reaction temperature = 298 K.

3.3.3. Reaction temperature

To understand the effect of the reaction temperature, we investigated the dechlorination of 2,4-D at temperatures ranging from 278 to 298 K, respectively. Considering that the temperature under normal conditions is 298 K [39], and wastewater has a temperature range of 5°C–25°C [40], the experiment was performed at <298 K. As shown in Fig. 5a, the removal efficiency of 2,4-D increased upon increasing the temperature from 278 to 298 K. Correspondingly, the k_{obs} value increased from 0.018 to 0.062 min^{-1}, which can be explained by the fact that the mass transfer of 2,4-D and production of active atomic H* were accelerated upon increasing the reaction temperature [41–43].

The Arrhenius equation was used to establish the relationship between the observed rate constant and temperature, which can be described using Eq. (2), as follows:

$$\ln k_{obs} = \ln A - \frac{Ea}{RT} \quad (2)$$

where k_{obs} represents the measured observed rate constant (min^{-1}), A is the pre-exponential factor (min^{-1}), Ea is the apparent activation energy (J/mol), R is the universal gas constant and T is the absolute temperature (K).

A plot of lnk_{obs} vs. 1/T resulted in a linear relationship with the slope and intercept equal to −Ea/R and ln$A$, respectively, as shown in Fig. 5c. According to Fig. 5c, the Ea was calculated to be 42.33 × 10^3 J/mol [44,45].

3.3.4. Dissolved anions

The effects of various inorganic anions on the removal of 2,4-D were investigated in an attempt to evaluate the possible application of the technique. It has been demonstrated that Pd may suffer from deactivation and poisoning due to the presence of reduced sulfur compounds and Cl$^-$ ions [46–49]. Fig. 6a shows that SO_3^{2-} and S^{2-} have a significantly negative effect on the catalyst activity. With 1 mmol/L SO_3^{2-} or 1 mmol/L S^{2-}, the activity of the catalyst can be significantly reduced. The removal efficiency of 2,4-D was reduced to 45.7% and ~0.0% after 120 min of electrolysis. Poisoning by SO_3^{2-} and S^{2-} can be attributed to the adsorption of sulfur and the formation of Pd sulfide on the Pd surface [25,35,50]. Sulfur saturated Pd surface will hinder the passage of hydrogen atoms from the bulk to the surface as well as hydrogen adsorption inside

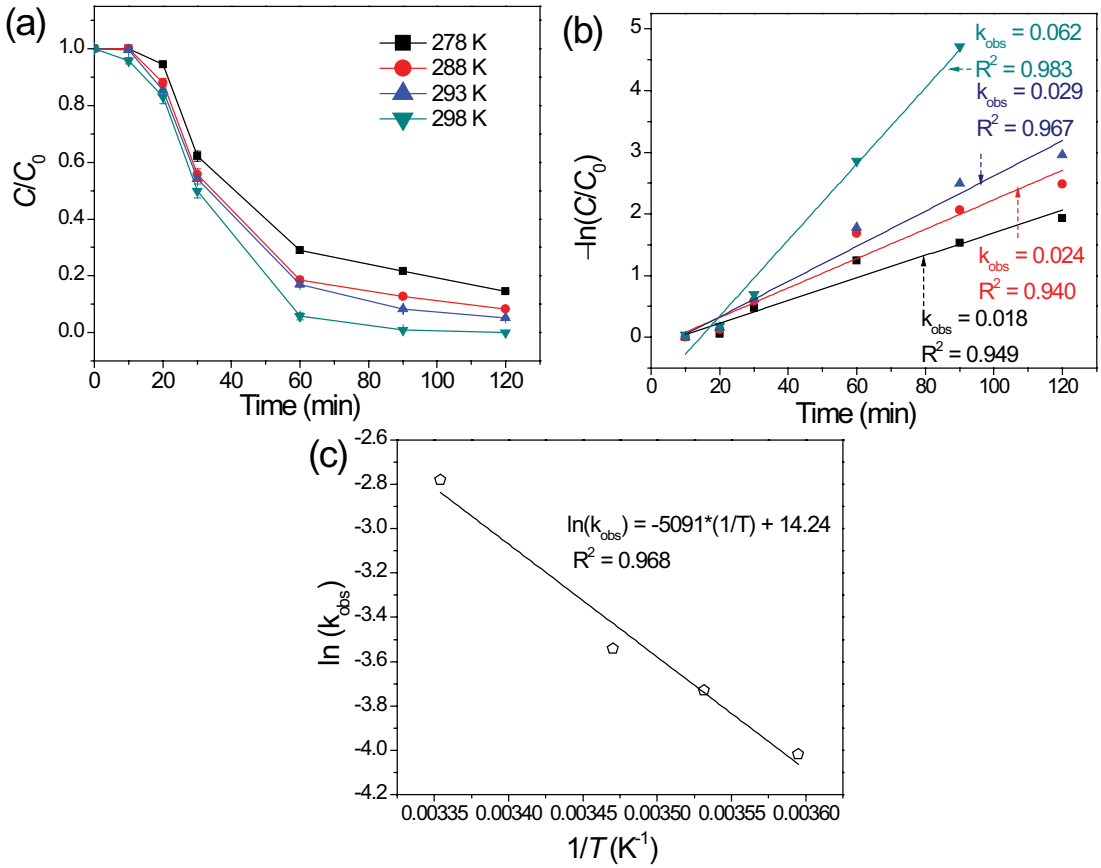

Fig. 5. (a) Effect of temperature on the dechlorination of 2,4-D. (b) Pseudo-first-order fitting and (c) Arrhenius plot of ln(k_{obs}) and 1/T using the Pd-Co_3O_4/Ni foam electrode. Experimental conditions: Pd loading = 0.47 mg/cm², Co_3O_4 loading = 0.51 mg/cm², initial 2,4-D concentration = 50 mg/L, Na_2SO_4 = 17 mmol/L, and applied current density = 1.50 mA/cm².

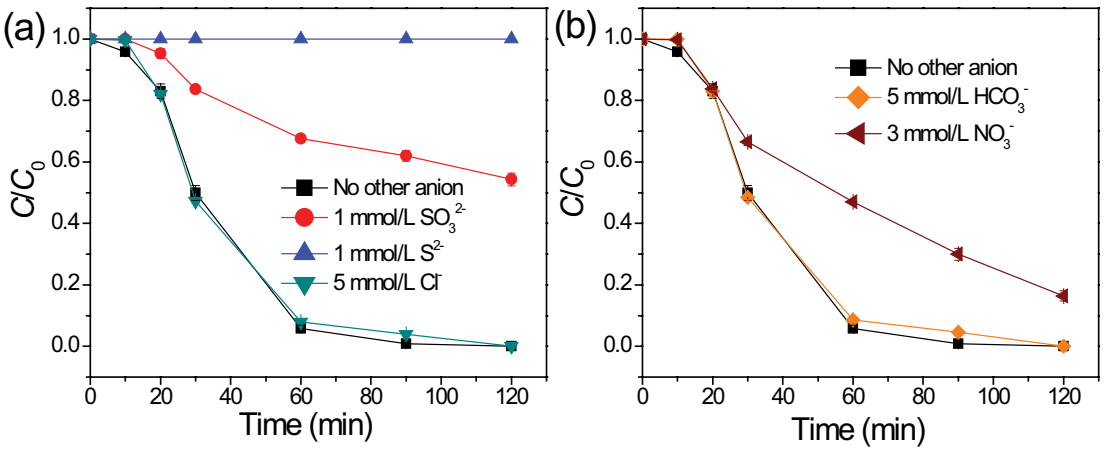

Fig. 6. Effect of dissolved anions (S^{2-}, SO_3^{2-}, Cl^-, NO_3^-, and HCO_3^-) on the dechlorination of 2,4-D using the Pd-Co_3O_4/Ni foam electrode. Experimental conditions: Pd loading = 0.47 mg/cm², Co_3O_4 loading = 0.51 mg/cm², initial 2,4-D concentration = 50 mg/L, Na_2SO_4 = 17 mmol/L, applied current density = 1.50 mA/cm², and reaction temperature = 298 K.

Pd lattice. The results also show that S^{2-} inhibits the dechlorination process more severely than SO_3^{2-}. In contrast, the additional addition of 5 mmol/L Cl^- showed no obvious negative effect on the dechlorination of 2,4-D. The Pd-Co_3O_4/Ni foam electrode exhibited good resistance to deactivation in the presence of Cl^-, which can be attributed to the formation of palladium oxide on the electrode surface, which has been previously discussed in detail by our group [26,51].

HCO_3^- and NO_3^- can inhibit the dechlorination reaction by competing with Cl-containing contaminants to consume

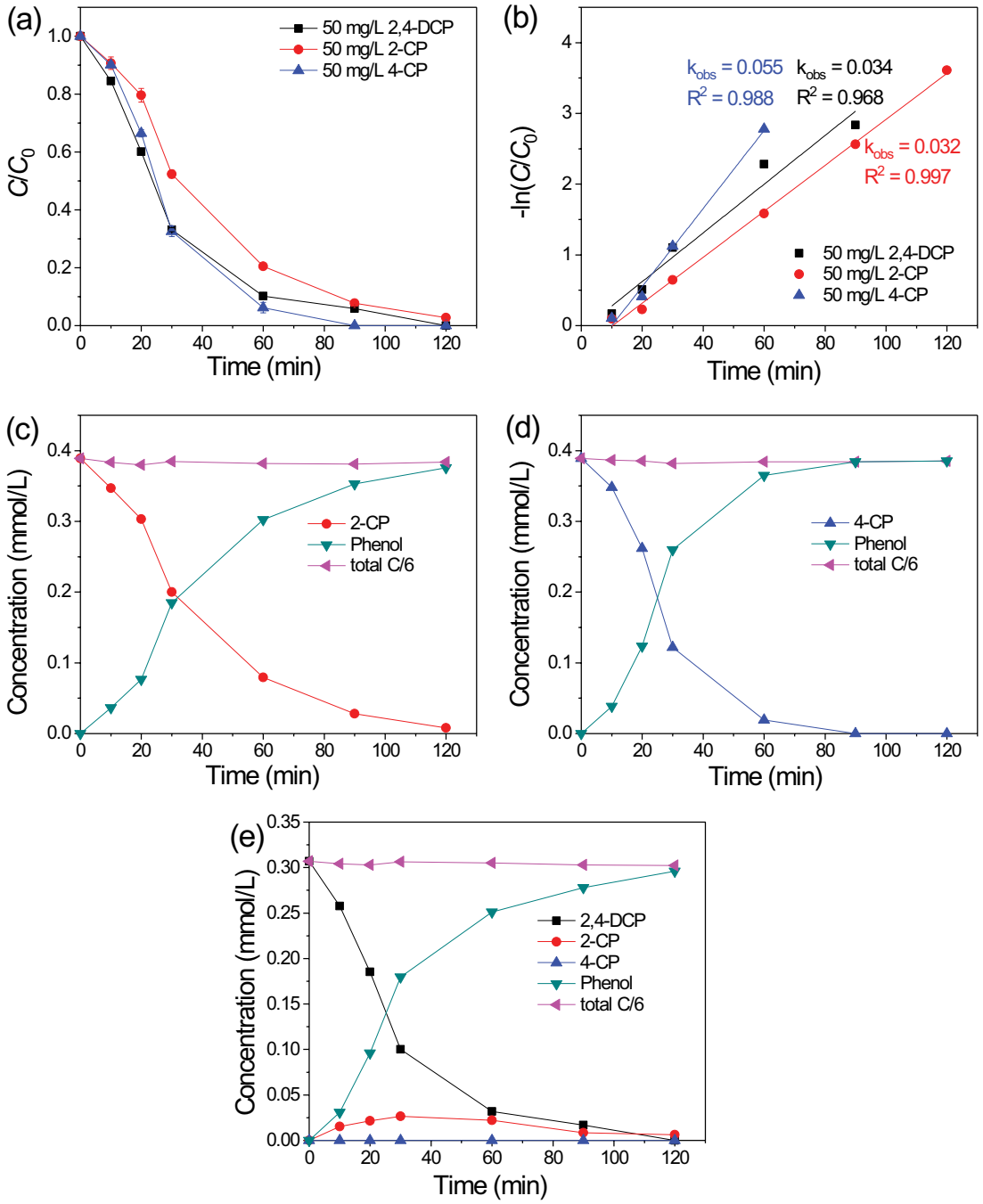

Fig. 7. (a) Dechlorination of 2,4-DCP, 2-CP and 4-CP. (b) Pseudo-first-order fitting of the Pd-Co_3O_4/Ni foam electrode. The time dependence of (c) 2-CP, final product and total carbon concentration, (d) 4-CP, final products and total carbon concentrations and (e) 2,4-DCP, intermediate, final product and total carbon concentration. Experimental conditions: Pd loading = 0.47 mg/cm², Co_3O_4 loading = 0.51 mg/cm², initial pollutant concentration = 50 mg/L, Na_2SO_4 = 17 mmol/L, applied current density = 1.50 mA/cm², and reaction temperature = 298 K.

H_2, as described in Eqs. (3) and (4) [50,52]. Thus, the effect of HCO_3^- and NO_3^- on the dechlorination of 2,4-D was also investigated, as shown in Fig. 6b. When 5 mmol/L HCO_3^- was present in the solution, no significant negative effect on the dechlorination of 2,4-D was observed. This may be due to the relatively slow reaction rate between HCO_3^- and H_2 when compared with the dechlorination reaction in this case. However, the adverse effect of NO_3^- could not be neglected due to the competing consumption of H_2 (Eq. (4)). When the NO_3^- concentration was 3 mmol/L, the removal efficiency toward 2,4-D reduced to 83.6% after 120 min.

$$HCO_3^- + H_2 \xleftrightarrow{Pd} HCO_2^- + H_2O \quad (3)$$

$$2NO_3^- + 5H_2 \xleftrightarrow{Pd} N_2 + 2OH^- + 4H_2O \quad (4)$$

3.4. Application of the dechlorination process toward other pollutants

Organic pollutants in the aquatic environment have become a ubiquitous and serious problem caused by industrial, domestic and environmental influences [53,54]. To confirm whether the Pd-Co_3O_4/Ni foam electrode can dechlorinate other COCs, the electrochemical dechlorination of 2,4-DCP, 2-CP, and 4-CP was performed under the same experimental conditions. As shown in Fig. 7a, the rapid dechlorination of these chlorophenol compounds was achieved and the removal of 2,4-DCP, 2-CP, and 4-CP reached ~100% after 120 min. After fitting with a pseudo-first-order kinetic model (Fig. 7b), the k_{obs} values obtained for the dechlorination of 2,4-DCP, 2-CP and 4-CP on the Pd-Co_3O_4/Ni foam electrode were 0.032, 0.034, and 0.055 min^{-1}, respectively. The final product of 2-CP and 4-CP electrochemical dechlorination only contained phenol (Figs. 7c and d). In comparison, the dechlorination of 2,4-DCP yielded a small amount of 2-CP accompanied with a large amount of phenol, and 4-PC could not be detected above the limit of determination, as shown in Fig. 7e. The facile removal of Cl from the 4-position compared to the 2-position was possibly due to the steric hindrance caused by the neighboring functional groups, which was in accordance with that reported in the literature [55,56]. The total carbon mass before and after the reaction remained stable during the entire reaction, providing evidence that the adsorption of the reactant or product on the electrode surface was negligible. These results demonstrate the excellent electroreduction ability of the Pd-Co_3O_4/Ni foam electrode towards other COCs.

3.5. Possible environmental application

We determined the applicability of the Pd-Co_3O_4/Ni foam electrode in a realistic water matrix, such as Hangzhou tap and river water. The initial 2,4-D concentration was adjusted to 2 mg/L. As shown in Fig. 8, approximately 83.6% and 71.8% of 2,4-D were removed after 60 min of electrolysis in Hangzhou tap and river water, respectively. Therefore, the Pd-Co_3O_4/Ni foam electrode maintained its high dechlorination efficiency for pollutants in an actual water body.

4. Conclusions

In conclusion, the Pd-Co_3O_4/Ni foam electrode prepared with a Pd loading of 0.47 mg/cm^2 and Co_3O_4 loading of 0.51 mg/cm^2 showed the best composition towards the electrochemical dechlorination of 2,4-D. Our experiments showed that the optimum utilization rate of active atomic H* was obtained at a current density of 1.50 mA/cm^2, an initial 2,4-D concentration of 50 mg/L and reaction temperature of 298 K. The Ea value was determined to be 42.33 × 10^3 J/mol based on the temperature dependence. 5 mmol/L HCO_3^- and Cl^- have a negligible effect on the dechlorination process. Nonetheless, a total of 1 mmol/L SO_3^{2-}, 1 mmol/L S^{2-} and 3 mmol/L NO_3^- have a significant negative effect on the electrocatalytic dechlorination reaction. The Pd-Co_3O_4/Ni foam electrode can also be applied to dechlorinate other chlorophenol compounds. The electrocatalytic dechlorination of 2,4-D in a realistic water matrix showed that the Pd-Co_3O_4/Ni foam electrode has broad practical application prospects.

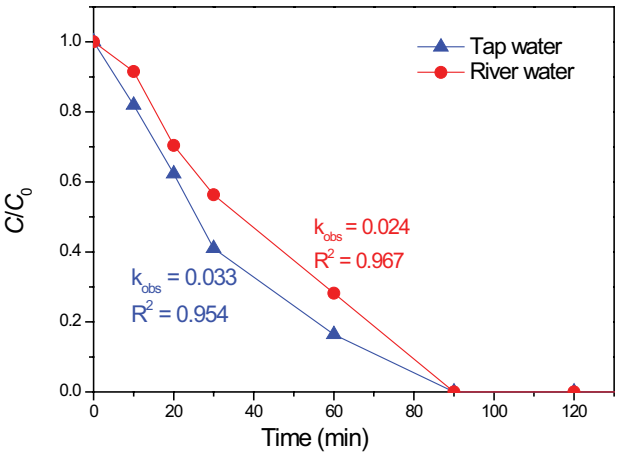

Fig. 8. Dechlorination of 2,4-D in tap and river water using the Pd-Co_3O_4/Ni foam electrode. Experimental conditions: Pd loading = 0.47 mg/cm^2, Co_3O_4 loading = 0.51 mg/cm^2, initial 2,4-D concentration = 2 mg/L, applied current density = 1.50 mA/cm^2, and reaction temperature = 298 K.

Acknowledgments

This work was supported by the National Natural Science Foundation of China (Grant 21477117) and the Zhejiang Provincial Natural Science Foundation of China (Grants LZ18B070001, LGF18E080017, and LR14E080001).

References

[1] D.E. Goggin, G.L. Nealon, G.R. Cawthray, A. Scaffidi, M.J. Howard, S.B. Powles, G.R. Flematti, Identity and activity of 2,4-dichlorophenoxyacetic acid metabolites in wild radish (raphanus raphanistrum), J. Agric. Food. Chem., 66 (2018) 13378–13385.
[2] S. Cenkci, M. Yildiz, I.H. Cigerci, A. Bozdag, H. Terzi, E.S.A. Terzi, Evaluation of 2,4-D and dicamba genotoxicity in bean seedlings using comet and RAPD assays, Ecotoxicol. Environ. Saf., 73 (2010) 1558–1564.
[3] P.H. Chen, Y.M. Shi, P.P. Niu, T. Wang, X.Q. Li, H.L. Jiang, W.Q. Zhou, H.Y. Shu, J.Z. Chen, E.Z. Tian, Highly sensitive detection of 4-NP in real water with long stability and high anti-inteference ability based on GO-Ag_2CrO_4/GCE, J. Taiwan Inst. Chem. Eng., 97 (2019) 128–136.
[4] P.H. Chen, Y.M. Shi, X.Q. Li, T. Wang, M.H. Zhou, E.Z. Tian, W.L. Wang, H.L. Jiang, H.Y. Shu, Highly effective detection of 4-nitrophenol by tremella-like indium silver sulfide modified GCE, Int. J. Electrochem. Sci., 13 (2018) 6158–6168.
[5] L. Yang, W. Sun, S. Luo, Y. Luo, White fungus-like mesoporous Bi_2S_3 ball/TiO_2 heterojunction with high photocatalytic efficiency in purifying 2,4-dichlorophenoxyacetic acid/Cr(VI) contaminated water, Appl. Catal., B, 156 (2014) 25–34.
[6] J.Y. Ma, X.C. Quan, Z.F. Yang, A.J. Li, Biodegradation of a mixture of 2,4-dichlorophenoxyacetic acid and multiple chlorophenols by aerobic granules cultivated through plasmid pJP4 mediated bioaugmentation, Chem. Eng. J., 181 (2012) 144–151.
[7] C. Zhu, J. Xu, S. Song, J. Wang, Y. Li, R. Liu, Y. Shen, TiO_2 quantum dots loaded sulfonated graphene aerogel for effective adsorption-photocatalysis of PFOA, Sci. Total Environ., 698 (2020) 134275.

[8] O. Garcia, E. Isarain-Chavez, S. Garcia-Segura, E. Brillas, J.M. Peralta-Hernandez, Degradation of 2,4-dichlorophenoxyacetic acid by electro-oxidation and electro-Fenton/BDD processes using a pre-pilot plant, Electrocatalysis, 4 (2013) 224–234.
[9] S. Sanches, M.T. Barreto Crespo, V.J. Pereira, Drinking water treatment of priority pesticides using low pressure UV photolysis and advanced oxidation processes, Water Res., 44 (2010) 1809–1818.
[10] T. Zeng, S.Q. Li, Y. Shen, H.Y. Zhang, H.R. Feng, X.L. Zhang, L.X.Y. Li, Z.W. Cai, S. Song, Sodium doping and 3D honeycomb nanoarchitecture: Key features of covalent triazine-based frameworks (CTF) organocatalyst for enhanced solar-driven advanced oxidation processes, Appl. Catal., B, 257 (2019) 117915.
[11] Y. Shen, C. Zhu, S. Song, T. Zeng, L. Li, Z. Cai, Defect-abundant covalent triazine frameworks as sunlight-driven self-cleaning adsorbents for volatile aromatic pollutants in water, Environ. Sci. Technol., 53 (2019) 9091–9101.
[12] G.H. Zhao, Y.G. Zhang, Y.Z. Lei, B.Y. Lv, J.X. Gao, Y.A. Zhang, D.M. Li, Fabrication and electrochemical treatment application of a novel lead dioxide anode with superhydrophohic surfaces, high oxygen evolution potential, and oxidation capability, Environ. Sci. Technol., 44 (2010) 1754–1759.
[13] E. Guinea, F. Centellas, E. Brillas, P. Canizares, C. Saez, M.A. Rodrigo, Electrocatalytic properties of diamond in the oxidation of a persistant pollutant, Appl. Catal., B, 89 (2009) 645–650.
[14] Z.Q. He, L.Y. Zhan, Q. Wang, S. Song, J.M. Chen, K.R. Zhu, X.H. Xu, W.P. Liu, Increasing the activity and stability of chemi-deposited palladium catalysts on nickel foam substrate by electrochemical deposition of a middle coating of silver, Sep. Purif. Technol., 80 (2011) 526–532.
[15] Z.Q. He, Q.W. Jian, J.T. Tang, T. Xu, J.L. Xu, Z.S. Yu, J.M. Chen, S. Song, Improvement of electrochemical reductive dechlorination of 2,4-dichlorophenoxyacetic acid using palladium catalysts prepared by a pulsed electrodeposition method, Electrochim. Acta, 222 (2016) 488–498.
[16] R. Mao, X. Zhao, H.C. Lan, H.J. Liu, J.H. Qu, Efficient electrochemical reduction of bromate by a Pd/rGO/CFP electrode with low applied potentials, Appl. Catal., B, 160 (2014) 179–187.
[17] Z.R. Sun, X.F. Wei, X. Hu, K. Wang, H.T. Shen, Electrocatalytic dechlorination of 2,4-dichlorophenol in aqueous solution on palladium loaded meshed titanium electrode modified with polymeric pyrrole and surfactant, Colloids Surf., A, 414 (2012) 314–319.
[18] S. Song, Q.X. Liu, J.H. Fang, W.T. Yu, Enhanced electrocatalytic dechlorination of 2,4-dichlorophenoxyacetic acid on in situ prepared Pd-anchored $Ni(OH)_2$ bifunctional electrodes: synergistic effect between H* formation on $Ni(OH)_2$ and dechlorination steps on Pd, Catal. Sci. Technol., 9 (2019) 5130–5141.
[19] K.R. Zhu, S.A. Baig, J. Xu, T.T. Sheng, X.H. Xu, Electrochemical reductive dechlorination of 2,4-dichlorophenoxyacetic acid using a palladium/nickel foam electrode, Electrochim. Acta, 69 (2012) 389–396.
[20] B.B. Huang, A.A. Isse, C. Durante, C.H. Wei, A. Gennaro, Electrocatalytic properties of transition metals toward reductive dechlorination of polychloroethanes, Electrochim. Acta, 70 (2012) 50–61.
[21] J.S. Zhou, Z.M. Lou, K.L. Yang, J. Xu, Y.Z. Li, Y.L. Liu, S.A. Baig, X.H. Xu, Electrocatalytic dechlorination of 2,4-dichlorobenzoic acid using different carbon-supported palladium moveable catalysts: adsorption and dechlorination activity, Appl. Catal., B, 244 (2019) 215–224.
[22] L. Altamar, L. Fernandez, C. Borras, J. Mostany, H. Carrero, B. Scharifker, Electroreduction of chloroacetic acids (mono-, di- and tri-) at polyNi(II)-tetrasulfonated phthalocyanine gold modified electrode, Sens. Actuators, B, 146 (2010) 103–110.
[23] W.C. Conner, J.L. Falconer, Spillover in heterogeneous catalysis, Chem. Rev., 95 (1995) 759–788.
[24] J.S. Zhou, Z. Lou, J. Xu, X.X. Zhou, K.L. Yang, X.Y. Gao, Y.L. Zhang, X.H. Xu, Enhanced electrocatalytic dechlorination by dispersed and moveable activated carbon supported palladium catalyst, Chem. Eng. J., 358 (2019) 1176–1185.
[25] C. Sun, Z.M. Lou, Y. Liu, R.Q. Fu, X.X. Zhou, Z. Zhang, S.A. Baig, X.H. Xu, Influence of environmental factors on the electrocatalytic dechlorination of 2,4-dichlorophenoxyacetic acid on nTiN doped Pd/Ni foam electrode, Chem. Eng. J., 281 (2015) 183–191.
[26] Q.X. Liu, Y.T. Shen, S. Song, Z.Q. He, Enhanced electrocatalytic hydrodechlorination of 2,4-dichlorophenoxyacetic acid by a Pd-Co_3O_4/Ni foam electrode, RSC Adv., 9 (2019) 12124–12133.
[27] L.M. Yang, Z.L. Chen, D. Cui, X.B. Luo, B. Liang, L.X. Yang, T. Liu, A.J. Wang, S.L. Luo, Ultrafine palladium nanoparticles supported on 3D self-supported Ni foam for cathodic dechlorination of florfenicol, Chem. Eng. J., 359 (2019) 894–901.
[28] H. Wang, J.L. Wang, Comparative study on electrochemical degradation of 2,4-dichlorophenol by different Pd/C gas-diffusion cathodes, Appl. Catal., B, 89 (2009) 111–117.
[29] P.H. Shao, L. Ding, J.F. Luo, Y. Luo, D. You, Q.G. Zhang, X.B. Luo, Lattice-defect-enhanced adsorption of arsenic on zirconia nanospheres: a combined experimental and theoretical study, ACS Appl. Mater. Interfaces, 11 (2019) 29736–29745.
[30] L.M. Yang, G.P. Yi, Y.A. Hou, H.Y. Cheng, X.B. Luo, S.G. Pavlostathis, S.L. Luo, A.J. Wang, Building electrode with three-dimensional macroporous interface from biocompatible polypyrrole and conductive graphene nanosheets to achieve highly efficient microbial electrocatalysis, Biosens. Bioelectron., 141 (2019) 111444.
[31] F. Yang, Y. Li, T. Liu, K. Xu, L. Zhang, C. Xu, J. Gao, Plasma synthesis of Pd nanoparticles decorated-carbon nanotubes and its application in Suzuki reaction, Chem. Eng. J., 226 (2013) 52–58.
[32] H. Zhao, J. Yang, L. Wang, C. Tian, B. Jiang, H. Fu, Fabrication of a palladium nanoparticle/graphene nanosheet hybrid via sacrifice of a copper template and its application in catalytic oxidation of formic acid, Chem. Commun., 47 (2011) 2014–2016.
[33] J.H. Zhong, A.L. Wang, G.R. Li, J.W. Wang, Y.N. Ou, Y.X. Tong, Co_3O_4/$Ni(OH)_2$ composite mesoporous nanosheet networks as a promising electrode for supercapacitor applications, J. Mater. Chem., 22 (2012) 5656–5665.
[34] C. Yuan, L. Yang, L. Hou, L. Shen, X. Zhang, X.W. Lou, Growth of ultrathin mesoporous Co_3O_4 nanosheet arrays on Ni foam for high-performance electrochemical capacitors, Energy Environ. Sci., 5 (2012) 7883–7887.
[35] W.J. Xie, S.H. Yuan, X.H. Mao, W. Hu, P. Liao, M. Tong, A.N. Alshaulabkeh, Electrocatalytic activity of Pd-loaded Ti/TiO_2 nanotubes cathode for TCE reduction in groundwater, Water Res., 47 (2013) 3573–3582.
[36] X.Q. Li, Y.M. Shi, P.H. Chen, Y.C. Bai, G.F. Li, H.Y. Shu, D.Z. Chen, S.J. Li, H.L. Jiang, Multifunctional electrochemical application of a novel 3D $AgInS_2$/rGO nanohybrid for electrochemical detection and HER, J. Chem. Technol. Biotechnol., 94 (2019) 3713–3724.
[37] X.F. Wei, X. Wan, Z.R. Sun, J. Miao, R. Zhang, Q. Niu, Understanding electrocatalytic hydrodechlorination of chlorophenols on palladium-modified cathode in aqueous solution, ACS Omega, 3 (2018) 5876–5886.
[38] B. Yang, G. Yu, D.M. Shuai, Electrocatalytic hydrodechlorination of 4-chlorobiphenyl in aqueous solution using palladized nickel foam cathode, Chemosphere, 67 (2007) 1361–1367.
[39] Q. Qiu, W. Jiang, S. Shen, X. Zhu, X. Mu, Numerical investigation on characteristics of falling film in horizontal-tube falling film evaporator, Desal. Wat. Treat., 55 (2015) 3247–3252.
[40] Z. Zheng, Y. Li, J. Li, Y. Zhang, W. Bian, J. Wei, B. Zhao, J. Yang, Effects of carbon sources, COD/NO_2^-–N ratios and temperature on the nitrogen removal performance of the simultaneous partial nitrification, anammox and denitrification (SNAD) biofilm, Water Sci. Technol., 75 (2017) 1712–1721.
[41] A. Brisse, J. Schefold, M. Zahid, High temperature water electrolysis in solid oxide cells, Int. J. Hydrogen Energy, 33 (2008) 5375–5382.
[42] F. He, D.Y. Zhao, Hydrodechlorination of trichloroethene using stabilized Fe-Pd nanoparticles: reaction mechanism and

effects of stabilizers, catalysts and reaction conditions, Appl. Catal., B, 84 (2008) 533–540.
[43] J. Xu, L.S. Tan, S.A. Baig, D.L. Wu, X.S. Lv, X.H. Xu, Dechlorination of 2,4-dichlorophenol by nanoscale magnetic Pd/Fe particles: effects of pH, temperature, common dissolved ions and humic acid, Chem. Eng. J., 231 (2013) 26–35.
[44] J.P. Wang, Y.M. Zhang, J. Huang, T. Liu, Kinetic and mechanism study of vanadium acid leaching from black shale using microwave heating method, JOM, 70 (2018) 1031–1036.
[45] V.V. Zhukov, A. Laari, M. Lampinen, T. Koiranen, A mechanistic kinetic model for direct pressure leaching of iron containing sphalerite concentrate, Chem. Eng. Res. Des., 118 (2017) 131–141.
[46] P. Albers, J. Pietsch, S.F. Parker, Poisoning and deactivation of palladium catalysts, J. Mol. Catal. A: Chem., 173 (2001) 275–286.
[47] T.C. Yu, H. Shaw, The effect of sulfur poisoning on methane oxidation over palladium supported on gamma-alumina catalysts, Appl. Catal., B, 18 (1998) 105–114.
[48] T.T. Lim, B.W. Zhu, Effects of anions on the kinetics and reactivity of nanoscale Pd/Fe in trichlorobenzene dechlorination, Chemosphere, 73 (2008) 1471–1477.
[49] C. Schuth, S. Disser, F. Schuth, M. Reinhard, Tailoring catalysts for hydrodechlorinating chlorinated hydrocarbon contaminants in groundwater, Appl. Catal., B, 28 (2000) 147–152.
[50] G.V. Lowry, M. Reinhard, Pd-catalyzed TCE dechlorination in groundwater: solute effects, biological control, and oxidative catalyst regeneration, Environ. Sci. Technol., 34 (2000) 3217–3223.
[51] N.S. Babu, N. Lingaiah, P.S.S. Prasad, Characterization and reactivity of Al_2O_3 supported Pd-Ni bimetallic catalysts for hydrodechlorination of chlorobenzene, Appl. Catal., B, 111 (2012) 309–316.
[52] G.V. Lowry, M. Reinhard, Pd-catalyzed TCE dechlorination in water: effect of [H_2] (aq) and H_2-utilizing competitive solutes on the TCE dechlorination rate and product distribution, Environ. Sci. Technol., 35 (2001) 696–702.
[53] P.H. Shao, J.Y. Tian, X.G. Duan, Y. Yang, W.X. Shi, X.B. Luo, F.Y. Cui, S.L. Luo, S.B. Wang, Cobalt silicate hydroxide nanosheets in hierarchical hollow architecture with maximized cobalt active site for catalytic oxidation, Chem. Eng. J., 359 (2019) 79–87.
[54] P.H. Shao, J.Y. Tian, F. Yang, X.G. Duan, S.S. Gao, W.X. Shi, X.B. Luo, F.Y. Cui, S.L. Luo, S.B. Wang, Identification and regulation of active sites on nanodiamonds: establishing a highly efficient catalytic system for oxidation of organic contaminants, Adv. Funct. Mater., 28 (2018) 1705295.
[55] W.Y. Fu, K.F. Wang, X.S. Lv, H.L. Fu, X.G. Dong, L. Chen, X.M. Zhang, G.M. Jiang, Palladium nanoparticles assembled on titanium nitride for enhanced electrochemical hydrodechlorination of 2,4-dichlorophenol in water, Chin. J. Catal., 39 (2018) 693–700.
[56] J. Xu, Z. Cao, X. Liu, H. Zhao, X. Xiao, J.P. Wu, X.H. Xu, J.L. Zhou, Preparation of functionalized Pd/Fe-Fe_3O_4@MWCNTs nanomaterials for aqueous 2,4-dichlorophenol removal: Interactions, influence factors, and kinetics, J. Hazard. Mater., 317 (2016) 656–666.